ISSN: 2357-0547 (Print)
ISSN: 2357-0539 (Online)

Research Article / JAPR / Sec. B
Akinwumi et al., 2022, 6 (3), **107-122**

Journal of Advanced Pharmacy Research

Section B: Pharmaceutical Analytical & Organic Chemistry, Medicinal & Biochemistry

In silico Studies of Bioactive Compounds Selected from Four African Plants with Inhibitory Activity Against *Plasmodium falciparum* Dihydrofolate Reductase-Thymidylate Synthase (*pf*DHFR-TS)

Ishola A. Akinwumi [1]*, Ayodele I. Faleti[1], Adefolarin P. Owojuyigbe[1], Faridat M. Raji[2], Michael M. Alaka[3]

[1]Department of Chemistry, School of Physical Sciences, Federal University of Technology, Akure, Ondo State, Nigeria, P.M.B.704. [2]Department of Biology, School of Life Sciences, Federal University of Technology, Akure, Ondo State, Nigeria, P.M.B.704. [3]Department of Integrated Science, Lagos State University of Education Otto/Ijanikan, Lagos State, Nigeria, P.M.B.007.

***Corresponding authors:** Ishola A. Akinwumi, [1]Department of Chemistry, School of Physical Sciences, Federal University of Technology, Akure, Ondo State, Nigeria, P.M.B.704. Tel. +2348101809859*
Email address: akinwumiche153954@futa.edu.ng; akinwumiishola5000@gmail.com

Submitted on: 20-05-2022; Revised on: 30-06-2022; Accepted on: 02-07-2022

To cite this article: Akinwumi, I A.; Faleti, A. I.; Owojuyigbe, A. P.; Raji, F. M.; Alaka, O. M. *In silico* Studies of Bioactive Compounds Selected from Four African Plants with Inhibitory Activity Against *Plasmodium falciparum* Dihydrofolate Reductase-Thymidylate Synthase (*pf*DHFR-TS). *J. Adv. Pharm. Res.* **2022**, *6* (3), 107-122. DOI: 10.21608/aprh.2022.139794.1175

ABSTRACT

Objective: This present study aims to assess *in silico* inhibitory potentials of bioactive compounds present in *Vernonia amygdalina* (Bitter leaf), *Cymbopogon citratus* (Lemongrass), *Azadirachta indica* (Neem leaf), and *Carica papaya* (Pawpaw leaf) against *Plasmodium falciparum* Dihydrofolate reductase-thymidylate synthase (*pf*DHFR-TS) via binding at their active sites. **Methods**: *In silico* methods were used in this study. Twenty (20) bioactive compounds were selected from *Vernonia amygdalina*, *Cymbopogon citratus*, *Azadirachta indica*, and *Carica papaya.* Artemether and Lumefantrine were used as the control drugs. The PubChem identification number (PID), the 3D structure in structure data format (SDF), and the canonical SMILES of the bioactive compounds and the control drugs were obtained using the PubChem online server. The crystal structure of *pf*DHFR-TS was retrieved from the protein data bank. Drug-likeness of the selected bioactive compounds was assessed using the SwissADME online server. The successful compounds were docked into the protein's active site using AutoDock Vina docking software. The docked complexes were analyzed using proteins plus and protein-ligand interaction profiler web server. The bioactivity of the ligands was determined using the Molinspiration online server. ADMETlab online tool was used to determine the ligands' absorption, distribution, metabolism, excretion, and toxicity (ADMET) characteristics. **Results:** The drug-likeness screening indicated that eleven (11) out of the twenty bioactive compounds violated two or more of the five rules (Lipinski's, Ghose's, Veber's, Egan's, and Muegge's rules). The control drug Artemether didn't violate any rule, while Lumefantrine violated four out of the five rules. The molecular docking revealed that Nimbolide, Vernomygdin, Luteolin, and Emetine from *Azadirachta indica* (Neem leaf), *Vernonia amygdalina* (Bitter leaf), and *Carica papaya* (Pawpaw leaf) have binding energies of -10.1 kcal/mol, -9.2 kcal/mol, -8.6 kcal/mol, and -9.2 kcal/mol respectively, which are better than the binding energies of Artemether and Lumefantrine (-8.2 kcal/mol, and -7.6 kcal/mol). Thus, these bioactive compounds' binding energies indicate the binding affinity with *pf*DHFR-TS protein, suggesting that the bioactive compounds may possess a biological activity against malarial. The best

four ligands, Nimbolide, Vernomygdin, Luteolin, and Emetine, also showed excellent ADMET properties. **Conclusion:** Conclusively, the *in silico* analysis proposes that Nimbolide, Vernomygdin, Luteolin, and Emetine from *Azadirachta indica* (Neem leaf), *Vernonia amygdalina* (Bitter leaf), and *Carica papaya* (Pawpaw leaf) prove to be probable antimalarial drugs, and show better docking with the target protein compared to Artemether and Lumefantrine. To validate this study, *an in-vitro* and *in vivo* study is recommended to further this study for validation of the hit compounds, as *in silico* methods only predict the activity of these bioactive compounds.

Keywords: *Bioactive compounds; ADMET; Plasmodium falciparum; In silico.*

INTRODUCTION

Malaria is an endemic disease that affects many people in most tropical countries (Africa, Asia, and Latin America)[1]. *Plasmodium falciparum*, a *Plasmodium* genus protozoan, is the cause of the disease[2]. According to statistics, roughly half of the world's population is at risk of contracting malaria, and malaria alone is responsible for 1 to 2 million annual deaths (mostly among African children)[2]. Because no vaccine has yet been released, and the disease-causing parasites have developed resistance to existing chemotherapies[3]. One promising strategy for combating malaria is to look for new vaccines and drugs[4]. Malaria is a significant challenge due to antimalarial drug resistance[5]. Malaria endemic countries have changed therapeutic policies, shifting from monotherapy to combination therapy, artemisinin-based combination therapies (ACT), but artemisinin resistance in *P. falciparum* has been reported in Southeast Asia[5]. The known protein targets provide a clear understanding of the mechanism of action of each antimalarial target. Quinoline derivatives act on *Plasmodium* by accumulating in the food vacuoles in parasites, inhibiting heme detoxication, and inhibiting parasite respiration reaction in cytochrome BC1 complex, among other mechanisms. Antifolate derivatives inhibit dihydropteroate synthetase (*pf*DHPS), folic acid biosynthesis, and *Plasmodium falciparum* dihydrofolate reductase (*pf*DHFR). DHFR is a valid drug target for treating parasitic diseases such as malaria[6]. Malaria dihydrofolate reductase (DHFR) targets antifolate antimalarial drugs such as Pyrimethamine and Cycloguanil, the clinical efficacy of which has been compromised by resistance arising through resistance mutations at various sites on the enzyme. Plasmodium species' frequent drug resistance results in the evolution of novel drug candidates with novel modes of action. Malaria parasites require DHFR/folate to maintain a high replication rate, and they can also synthesize or scavenge folate newly synthesized[7, 8].

Furthermore, resistance to antimalarial drugs such as Chloroquine and Sulfadoxine-Pyrimethamine has been observed, particularly in malaria-endemic areas. Other antimalarial drugs with good efficacy include Mefloquine, Halofantrine, Atovaquone, and Proguanil, but there are drawbacks such as cost[9]. The emergence of antimalarial drug resistance has created an urgent need to develop new effective antimalarial compounds.

Developing a drug begins with identifying unmet medical needs, defined as dissatisfaction with current methods of diagnosis, therapy, and prevention. It then moves on to identifying biological targets for drug-able targets[9]. The discovery of a drug is both time-consuming and expensive. Incorporating computer-based methods such as docking techniques, pharmacophore-based searches, and neural networking[10] is one current approach for reducing the time and cost required to discover lead compounds that may inhibit or modulate known drug targets. Computer-based methods have also been used to predict drug molecules' likely metabolic pathways and pharmacokinetic profiles[11]. If a potential drug molecule enters the market, its absorption, distribution, metabolism, excretion, and toxicity (ADMET) profile must be known. As a result, assessing such information for lead compounds early on would aid in eliminating molecules with predicted uninteresting profiles, ultimately lowering the cost of drug discovery[6].

Natural products have been therapeutics for diseases for many years because they can produce certain biological activities and have drug-like properties[12]. The discovery of Artemisinin and Quinine is one example of successful drug development from natural products. These drugs have been widely used in antimalarial therapy[13]. *Vernonia amygdalina*, also known as the bitter leaf, is the most commonly cultivated species of the genus *Vernonia*, containing over 1,000 shrubs species[14]. It is produced and grown in many countries, primarily in savannah zones. Although *Vernonia amygdalina* is most commonly used for food, it has traditionally been used for medicinal properties. Traditional medicine practitioners also use it as an antihelminth, antimalarial, and laxative. Others use it as a digestive tonic, appetizer, febrifuge, and wound treatment[14]. The aqueous extract of *Vernonia amygdalina* leaves exhibits antimalarial activity against *Plasmodium falciparum*, *Plasmodium vivax*, *Plasmodium ovale*, and *Plasmodium malariae*, even though some of these strains are resistant to conventional antimalarial drugs[15]. So, in traditional practices, *Vernonia amygdalina* (Bitter leaf) treats

parasitic infections, particularly Malaria fever, the most common parasitic infection[15]. *Cymbopogon citratus* (Lemongrass) has become a cynosure of the modern medicinal system[16] due to many biologically active chemicals and therapeutic functions[17]. Lemongrass is reported to exhibit immunomodulatory, anti-inflammatory, antiviral, anticarcinogenic, antihyperglycaemic, antioxidant, antimalarial, antimutagenic, antimicrobial, and antiglycation properties. Lemongrass relieves headaches, body aches, nervous exhaustion, and stress-related conditions. Its infusions are frequently used to treat sore throats, laryngitis, and bronchitis[17].

Azadirachta indica (Neem) is a natural herb derived from the neem tree. The extract is derived from the tree's seeds and has a variety of traditional applications. However, neem is well-known for its pesticide and insecticidal properties. Neem leaves, flowers, seeds, fruits, roots, and bark have traditionally been used to treat inflammation, infections, fever, skin diseases, and dental disorder[18]. Immunomodulatory, anti-inflammatory, antihyperglycemic, antiulcer, antimalarial, antifungal, antibacterial, antiviral, antioxidant, antimutagenic, and anticarcinogenic properties have been demonstrated for neem leaf and its constituents[18].

Carica papaya (Pawpaw) has a wide distribution area due to its ease of cultivation, particularly in tropical regions. It is an American native plant introduced to India in the 16th century[19]. *Carica papaya* parts treat different illnesses, such as malaria, dengue fever, jaundice, and antiviral and immunomodulatory properties[19]. Flavonoids, alkaloids, phenolic compounds, carotene, lycopene, anthraquinone glycosides, and other chemicals are present in *Carica papaya*[20]. Teng *et al*.[21] conducted a scientific study on the potential antimalarial use of this plant, testing it against *P. falciparum* 3D7 and Dd2 strains. The results revealed antimalarial activity in the medium range. Carpaine, a member of the alkaloids family, is the compound responsible for this activity[20].

One option in the drug discovery process is to conduct an *in silico* study as a virtual screening method. The *in silico* method attempts to predict the orientation of molecular binding (ligands) with other molecules (protein targets) to form a stable complex. The *in silico* approach is frequently used to discover new drugs and has many advantages, including cost, time efficiency, and work effectiveness[22]. Thus, the present study aimed to assess the inhibitory potential of *Vernonia amygdalina* (Bitter leaf), *Cymbopogon citratus* (Lemongrass), *Azadirachta indica* (Neem leaf), and *Carica papaya* (Pawpaw leaf) against *Plasmodium falciparum* dihydrofolate reductase-thymidylate synthase (*pf*DHFR-TS) using an *in silico* approach.

MATERIAL AND METHODS

Ligand Selections

Vernonia amygdalina (Bitter leaf), *Cymbopogon citratus* (Lemongrass), *Azadirachta indica* (Neem leaf), and *Carica papaya* (Pawpaw leaf) are the four African plants used in this study. Twenty (20) bioactive compounds were selected from this compound using literature.[23-26]. Nicotinamide, Pyridoxine, Luteolin, Vernomygdin, and Vernomenin were chosen from *Vernonia amygdalin*[23]; Myrcene, Geraniol, Neral, Nerol, and Limonene were selected from *Cymbopogon citratus*[24], Nimbin, Nimbinene, Nimbolide, Desacetylnimbin, and Azadirone, were chosen from *Azadirachta indica*[25]; and Dehydrodocarpaine II, Emetine, Carpaine, (*R*)-prunasin, and Dehydrodocarpaine I were selected from *Carica papaya*[26]. Artemether and Lumefantrine were used as the control drugs. **Table 1** shows the bioactive compounds selected from the plants and the control drugs. In this study, a chemical repository server called PubChem web (https://pubchem.ncbi.nlm.nih.gov/compound/)[27] was used to obtain the PubChem identification number (PID), the 3D structure in structure data format (SDF), and the canonical SMILES of the bioactive compounds and the control drugs.

Protein targets selection

*pf*DHFR-TS is the target protein, and it was selected using literature[28]. The three-dimensional (3D) crystallographic structure of the target protein (PDB: 3UM8)[28] was downloaded from the research collaboratory of structural bioinformatics (RCSB) protein databank (www.rcsb.org)[29] and was saved in PDB format. **Figure 1** shows the structure of the protein *Plasmodium falciparum* dihydrofolate reductase-thymidylate synthase (*pf*DHFR-TS).

Protein targets preparation

The 3D structure of the target protein, *Plasmodium falciparum* dihydrofolate reductase-thymidylate synthase (*pf*DHFR-TS), was cleaned and prepared by separating it from the co-crystallized ligands using the UCSF-Chimera (version 1.13.1)[30]. UCSF-Chimera was used to remove water, add hydrogens, and assign Gasteiger-Huckel charges. The protein was minimized for molecular docking and was saved in PDB format.

Drug likeness screening

The drug-likeness screening of the twenty (20) bioactive compounds and two (2) control drugs was

carried out using the online server SwissADME (http://swissadme.ch/)[31] by using the canonical SMILES of the bioactive compounds and the control drugs. Nine (9) bioactive compounds violated only one of the five rules (Lipinski's[32-34], Ghose's[35], Veber's[36], Egan's[37], and Muegge's[38]) were subjected to molecular docking, and the control drugs were subjected to molecular docking.

Ligand Optimization and Molecular docking Molecular docking

Molecular docking of the ligands and the target protein was carried out using python prescription (PyRx) software[39]. The 3D structure of the downloaded ligands was uploaded sequentially into the Open babel integrated within PyRx (version 0.8), which were then optimized to their lowest energetic state for docking using merck molecular force field (MMFF94). The Ligands were then converted to AutoDock ligand format (PDBQT). The molecular docking study between the ligands and the protein receptors was carried out using the AutoDock Vina. The grid box with the center dimension (x: 29.0591, y: 14.8822, z: 53.6957), size (x: 62.7600, y: 93.2744, z: 56.8412 angstroms) was used to adjust the protein's active site. The following amino acids Ala16, Asp54, Phe58, Met55, Ser108, Ser111, Tyr170, Ser108, and Ile112 were selected from the literature and were found to be in be a binding region of the target protein and were used in the molecular docking[28, 40, 41]. The exhaustiveness of 10 was used in the molecular docking. The binding energy in kcal/mol was obtained from the molecular docking of each ligand and the protein. The PyRx was also used to convert the docked ligands and protein target from their PDBQT format into PDB format, and the files were saved for analysis and visualization.

Molecular interaction analysis

The ligands and target protein were analyzed to form protein-ligand complexes using the PyMOL© molecular graphics (version 2.4, 2010, Schrödinger LLC)[42], and the complexes were saved in PDB format. These complexes were then uploaded onto the protein-ligand interaction profiler (https://projects.biotec.tudresden.de/plip-web/plip)[43] and proteins plus (https://proteins.plus) [44, 45] web servers to determine their molecular interactions.

Prediction of bioactivity

The bioactivity of the ligands was determined using the Molinspiration online server (https://www.molinspiration.com)[46]. The activity score for GPCR ligand, ion channel modulator, nuclear receptor legend, a kinase inhibitor, protease inhibitor, and enzyme inhibitor of ligands was calculated using this online server. The following range is used to determine the bioactivity of organic compounds. If the bioactivity score is greater than 0 (>0), the compound is considered active. If it is between -5.0 and 0.0, the compound is moderately active. If the score is less than -5.0 (< -5.0), the compound is inactive[46].

Pharmacokinetics properties prediction

ADMETlab online tool (https://admetmesh.scbdd.com/service/evaluation/cal)[47] was used to determine the absorption, distribution, metabolism, excretion, and toxicity (ADMET) characteristics of the ligands obtained from the molecular docking, and the results were used to predict the pharmacokinetic properties of the ligands.

RESULTS

Drug likeness screening

The results of the drug-likeness screening for the bioactive compounds were obtained from the four African plants, *Vernonia amygdalina* (Bitter leaf), *Cymbopogon citratus* (Lemongrass), *Azadirachta indica* (Neem leaf), and *Carica papaya* (Pawpaw leaf) and the control drugs Artemether and Lumefantrine, which are used in malaria treatment, were presented in **Table 1**. This screening indicated eleven (11) out of the twenty bioactive compounds that violated two or more of the five rules (Lipinski's[32-34], Ghose's[35], Veber's[36], Egan's[37], and Muegge's[38]) were eliminated from the study for further analysis. The remaining nine (9) that passed the rules, and the two (2) control drugs were subjected to docking analysis with *pf*DHFR-TS.

Molecular docking and interaction of *Plasmodium falciparum* dihydrofolate reductase-thymidylate synthase (*pf*DHFR-TS) and ligands

The following are the amino acid residues present at the site for catalytic action in *pf*DHFR-TS, Ala16, Asp54, Phe58, Met55, Ser108, Ser111, Tyr170, Ser108, and Ile112[28, 40, 41]. The molecular docking results from this study are presented in **Table 2**. The study evaluated the binding efficiency, electrostatic energy, hydrophobic, and the hydrogen bond interaction between the compounds and *Plasmodium falciparum* dihydrofolate reductase-thymidylate synthase (*pf*DHFR-TS).

The shown results of the bioactive compounds from the four African plants in **Table 2** predict their binding affinity and suggest potential biological activity against the target protein *pf*DHFR-TS. Pyridoxine, Luteolin, Vernomygdin, and Vernomenin, are the bioactive compounds present in the bitter leaf. They bind to *pf*DHFR-TS with binding energies of -5.5, -8.6, -9.2, and -7.7 kcal/mol, respectively, while Vernomygdin has the lowest binding energy. The binding energies show

Table 1. Screening result of the bioactive compounds and the control drugs using the SwissADME online tool

S/N	Molecule	Formula	MW	XLOGP	TPSA	Lipinski #violations	Ghose #violations	Veber #violations	Egan #violations	Muegge #violations	Bioavailability Score
1	Nicotinamide	$C_6H_6N_2O$	122.12	-0.37	55.98	0	3	0	0	1	0.55
2	Pyridoxine	$C_8H_{11}NO_3$	169.18	-0.77	73.58	0	0	0	0	1	0.55
3	Luteolin	$C_{15}H_{10}O_6$	286.24	2.53	111.13	0	0	0	0	0	0.55
4	Vernomygdin	$C_{19}H_{24}O_7$	364.39	1.01	94.59	0	0	0	0	0	0.55
5	Vernomenin	$C_{15}H_{16}O_5$	276.28	1.34	72.83	0	0	0	0	0	0.55
6	Myrcene	$C_{10}H_{16}$	136.23	4.17	0	0	1	0	0	2	0.55
7	Geraniol	$C_{10}H_{18}O$	154.25	3.56	20.23	0	1	0	0	2	0.55
8	Neral	$C_{10}H_{16}O$	152.23	3.03	17.07	0	1	0	0	2	0.55
9	Nerol	$C_{10}H_{18}O$	154.25	3.56	20.23	0	1	0	0	2	0.55
10	Limonene	$C_{10}H_{16}$	136.23	4.57	0	0	1	0	0	2	0.55
11	Nimbin	$C_{30}H_{36}O_9$	540.6	2.28	118.34	1	3	0	0	0	0.55
12	Nimbinene	$C_{28}H_{34}O_7$	482.57	2.04	92.04	0	1	0	0	0	0.55
13	Nimbolide	$C_{27}H_{30}O_7$	466.52	2.17	92.04	0	0	0	0	0	0.55
14	Desacetylnimbin	$C_{28}H_{34}O_8$	498.56	1.71	112.27	0	1	0	0	0	0.55
15	Azadirone	$C_{28}H_{36}O_4$	436.58	5.72	56.51	1	1	0	1	1	0.55
16	Dehydrodocarpaine II	$C_{28}H_{46}N_2O_4$	474.68	5.66	77.32	0	3	0	0	1	0.55
17	Emetine	$C_{29}H_{40}N_2O_4$	480.64	4.74	52.19	0	3	0	0	0	0.55
18	Carpaine	$C_{28}H_{50}N_2O_4$	478.71	6.29	76.66	0	2	0	0	1	0.55
19	R-prunasin	$C_{14}H_{17}NO_6$	295.29	-0.71	123.17	0	1	0	0	0	0.55
20	Dehydrodocarpaine I	$C_{28}H_{48}N_2O_4$	476.69	5.97	76.99	0	2	0	0	1	0.55
21	Artemether	$C_{16}H_{26}O_5$	298.37	3.53	46.15	0	0	0	0	0	0.55
22	Lumefantrine	$C_{30}H_{32}Cl_3NO$	528.94	8.72	23.47	2	3	0	1	1	0.17

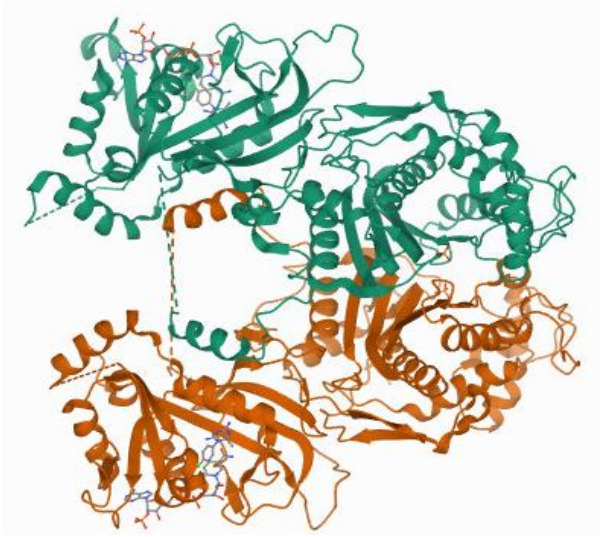

Figure 1. Structure of the protein *Plasmodium falciparum* dihydrofolate reductase-thymidylate synthase (*pf*DHFR-TS) [28] (Adopted from protein data bank).

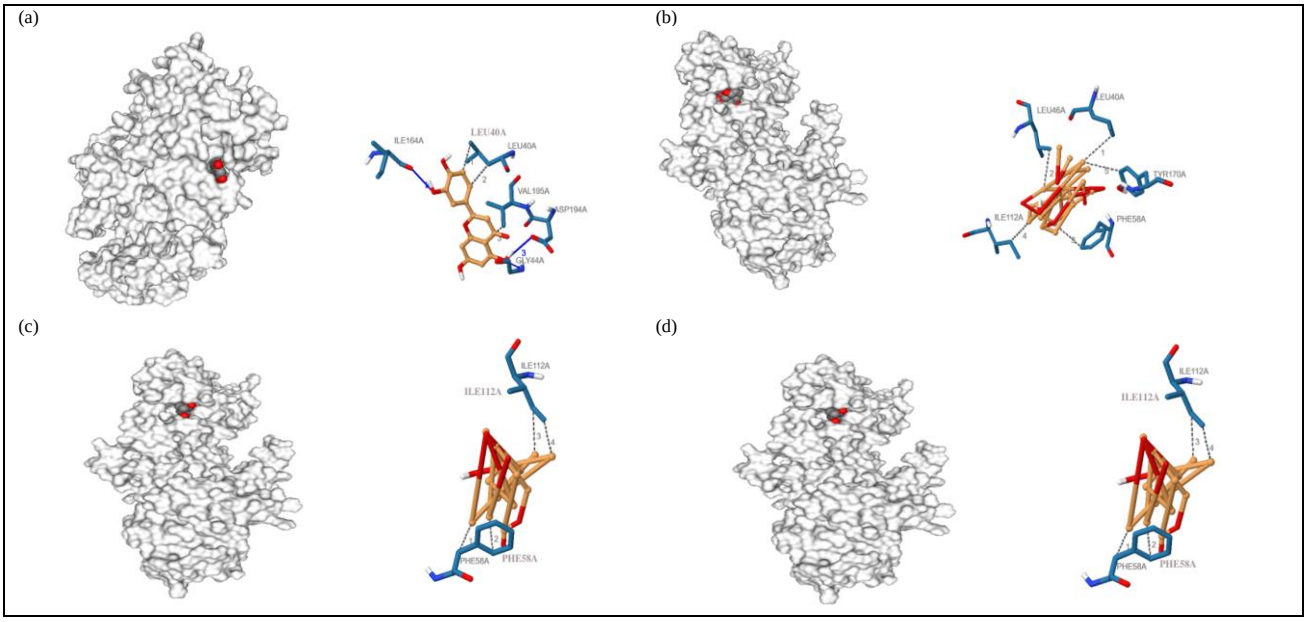

Figure 2. The binding configuration of Pyridoxine 2(a), Luteolin 2(b), Vernomygdin 2(c), and Vernomenin 2(d) in the *pf*DHFR-TS active site as obtained from molecular docking using AutoDock Vina. Binding interactions were analyzed using a protein-ligand interaction profiler. Blue dashed line - Hydrogen bond; Green dotted line – Pi stacking; Grey dotted line – Hydrophobic interaction.

how the bioactive compounds bind to the protein. **Figure 2a-d** illustrates the interaction of Pyridoxine, Luteolin**,** and Vernomygdin with *pf*DHFR-TS. Pyridoxine establishes one hydrogen bond with Asp54**.** Pyridoxine also interacts hydrophobically with Phe58. It also forms a π-stacking interaction with Phe58 (**Figure 2a**). Luteolin establishes three hydrogen bonds with Gly44, Ile164, and Asp194. Luteolin also interacts hydrophobically with Leu40 and Val195 (**Figure 2b**). Vernomygdin demonstrated hydrophobic interaction with Leu40, Leu46, Phe58, Ile112, and Tyr170 (**Figure 2c**). Vernomenin also interacts hydrophobically with Phe58 and Ile112 (Figure 2d). Nimbinene, Nimbolide, and Desacetylnimbin are the bioactive compounds in Neem leaf. They bind to *pf*DHFR-TS with -8.1, -10.1, and -8.1 kcal/mol, respectively, while Nimbolide has the highest binding affinity**. Figure 3a-c** shows the interaction of Nimbinene, Nimbolide, and Desacetylnimbin with *pf*DHFR-TS protein**.** Nimbinene establishes four hydrogen bonds with Lys373, Leu376, Arg377, and Tyr596**.** Nimbinene interacts hydrophobically with Leu376, Ile593, and Tyr596 (**Figure 3a**)**.** Nimbolide demonstrated hydrophobic interaction with Ala16, Leu46, Phe58, Ile112, Phe116, and Ile164 (**Figure 3b**). Desacetylnimbin interacted with Leu376 and Arg377 using hydrogen bonds and established hydrophobic interaction with Leu376, Ile380, and Ile593 (**Figure 3c**). Emetine and (*R*)-prunasin are the bioactive compounds present in pawpaw leaves. They bind to *pf*DHFR with -9.2 and -6.9 kcal/mol, respectively, while Emetine has the highest binding affinity**. Figure 4a-b** shows the interaction of Emetine and (*R*)-prunasin with *pf*DHFR**.** Emetine established hydrophobic interaction between Leu40, Leu46, Phe58, and Ile164 (**Figure 4a**). Using hydrogen bonds, (*R*)-prunasin interacted with Arg377, Gly378, Asn400, and Arg402**.** It also showed hydrophobic interaction with Ile379, Ile403, and Phe520, forming a π-stacking interaction with Phe520 (**Figure 4b**). Artemether and Lumefantrine are the control drugs used in this study with a binding energy of -8.2 and -7.6 kcal/mol**,** respectively**. Figure 5a-b** shows that both ligands penetrate deeply into the site for substrate metabolism in the target protein**.** Artemether interacts hydrophobically with Phe58 without a hydrogen bonding (**Figure 5a**)**.** Lumefantrine also interacts hydrophobically with Leu53, Tyr57, Ala60, Tyr214, Phe223, Ile225, and Tyr320, and it also forms a π-stacking interaction with Tyr 57 (**Figure 5b**).

Predicted bioactivity

The predicted bioactivity of the compounds and the control drugs are shown in **Table 3**. They include the activity score for GPCR ligand, ion channel modulator, nuclear receptor legend, kinase inhibitor, protease inhibitor, and enzyme inhibitor of ligands were calculated using this online server (https://www.molinspiration.com)[46]

Table 2. Analysis of molecular interactions for the bioactive compounds and the control drugs.

S/N	Plant source	Molecule	Binding energy (kcal/mol)	Number of hydrogen bond (s) formed	Residues involved in hydrogen bond formation (Å)	Residues involved in hydrophobic interaction (Å)	Residues involved in π-stacking (Å)	Residues involved in π-cation interaction (Å)
1	*Vernonia amygdalina*	Pyridoxine	-5.5	1	Asp54(3.57)	Phe58 (3.64)	Phe58(3.77)	
2		**Luteolin**	**-8.6**	**3**	**Gly44(2.10) Ile164(1.97) Asp194(2.86)**	**Leu40(3.56,3.43), Val195(3.48)**		
3		**Vernomygdin**	**-9.2**	**-**	-	**Leu40(3.72), Leu46(3.82), Phe58(3.76), Ile112(3.79) Tyr170(3.72)**		
4		Vernomenin	-7.7	-	-	Phe58(3.74,3.79) Ile112(3.73,3.71)		
5	*Azadirachta indica*	Nimbinene	-8.1	4	Lys373(2.02), Leu376(2.04), Arg377(2.29), Tyr596(1.99)	Leu376(3.28), Ile593(3.65,3.49), Tyr596(3.73,3.75)		
6		**Nimbolide**	**-10.1**			**Ala16(3.79), Leu46(3.66), Phe58(3.6,3.40,3.61) , Ile112(3.34), Phe116(3.37), Ile164(3.52)**		
7		Desacetylnimbin	-8.1	2	Leu376(2.16), Arg377(2.10)	Leu376(3.20), Ile380(3.94), Ile593(3.75,3.93)		
8	*Carica papaya*	**Emetine**	**-9.2**			**Leu40(3.54), Leu46(3.99,3.35), Phe58(3.61,3.76) Ile164(3.81)**		
9		*(R)*-prunasin	-6.9	6	Arg377(3.20,3.36) Gly378(2.13), Asn400(2.57,2.26) Arg402(2.15)	Ile403 (3.71,3.60) Ile379(3.54) Phe520(3.99)	Phe520(3.93)	
10		Artemether	-8.2	-		Phe58(3.6,3.66,3.81, 3.45)		
11		Lumefantrine	-7.6	-		Leu53(3.56), Tyr57(3.60,3.67), Ala60(3.72), Tyr214(3.74), Phe223(3.57), Ile225(3.63), Tyr320(3.58)	Tyr57(5.36,5.03)	

Table 3 shows the bioactivity scores of the compounds as well as all the control drugs. Pyridoxine, Luteolin, and Artemether have bioactivity scores between −5.0 and 0.0 for the GPCR ligand, indicating they are moderately active. Vernomygdin, Vernomenin, Nimbinene, Nimbolide, Desacetylnimbin, Emetine, (*R*)-prunasin, and Lumefantrine have bioactivity scores greater than 0.0 for GPCR ligand, which indicate that they are active. The Ion channel modulator bioactivity scores for Luteolin, Vernomenin, Artemether, and Lumefantrine range between −5.0 and 0.0, which suggests that they are moderately active, while Pyridoxine, Vernomygdin, Nimbinene, Nimbolide, Desacetylnimbin, Emetine, (*R*)-prunasin, and Lumefanthrine have bioactivity scores greater than 0.0 which indicate that they are highly active. Pyridoxine, Vernomygdin, Vernomenin, Nimbinene, Nimbolide, Desacetylnimbin, Emetine, (*R*)-prunasin, Artemether, and Lumefantrine have bioactivity scores between −5.0 and 0.0 for Kinase inhibitor which indicate that they are moderately active. Luteolin is the only compound with a bioactivity score greater than 0.0 for Kinase inhibitors, suggesting its high activity. Nuclear receptor ligand is another predicted bioactivity score for bioactive compounds and control drugs. Pyridoxine, Emetine, (*R*)-prunasin, Artemether, and Lumefantrine have bioactivity scores between −5.0 and 0.0 for nuclear receptor ligand, which indicate that they are moderately active. In contrast, Luteolin, Vernomygdin, Vernomenin, Nimbinene, Nimbolide, and Desacetylnimbin bioactivity scores are greater than 0.0, showing their high activity. Pyridoxine, Luteolin, Artemether, and Lumefantrine have bioactivity scores between −5.0 and 0.0 for Protease inhibitors, indicating they are moderately active. Vernomygdin, Vernomenin, Nimbinene, Nimbolide, Desacetylnimbin, Emetine, and (*R*)-prunasin have Protease inhibitor bioactivity scores greater than 0.0, which shows high bioactivity of the compounds.

Table 3. Predicted bioactivity score for bioactive compounds and control drugs

S/N	Compound name	GPCR ligand	Ion channel modulator	Kinase inhibitor	Nuclear receptor ligand	Protease inhibitor	Enzyme inhibitor
1	Pyridoxine	-0.39	0.35	-0.72	-0.77	-0.93	0.06
2	Luteolin	-0.02	-0.07	0.26	0.39	-0.22	0.28
3	Vernomygdin	0.30	0.17	-0.21	1.05	0.50	0.83
4	Vernomenin	0.05	-0.11	-0.44	1.07	0.04	0.64
5	Nimbinene	0.21	0.18	-0.30	0.37	0.04	0.33
6	Nimbolide	0.22	0.20	-0.36	0.32	0.04	0.36
7	Desacetylnimbin	0.31	0.21	-0.22	0.35	0.16	0.43
8	Emetine	0.22	0.10	-0.27	-0.20	0.08	-0.06
9	(*R*)-prunasin	0.26	0.03	-0.03	-0.07	0.21	0.60
10	Artemether	-0.05	-0.22	-0.44	-0.01	-0.07	0.45
11	Lumefantrine	0.17	-0.19	-0.15	0.01	-0.19	0.04

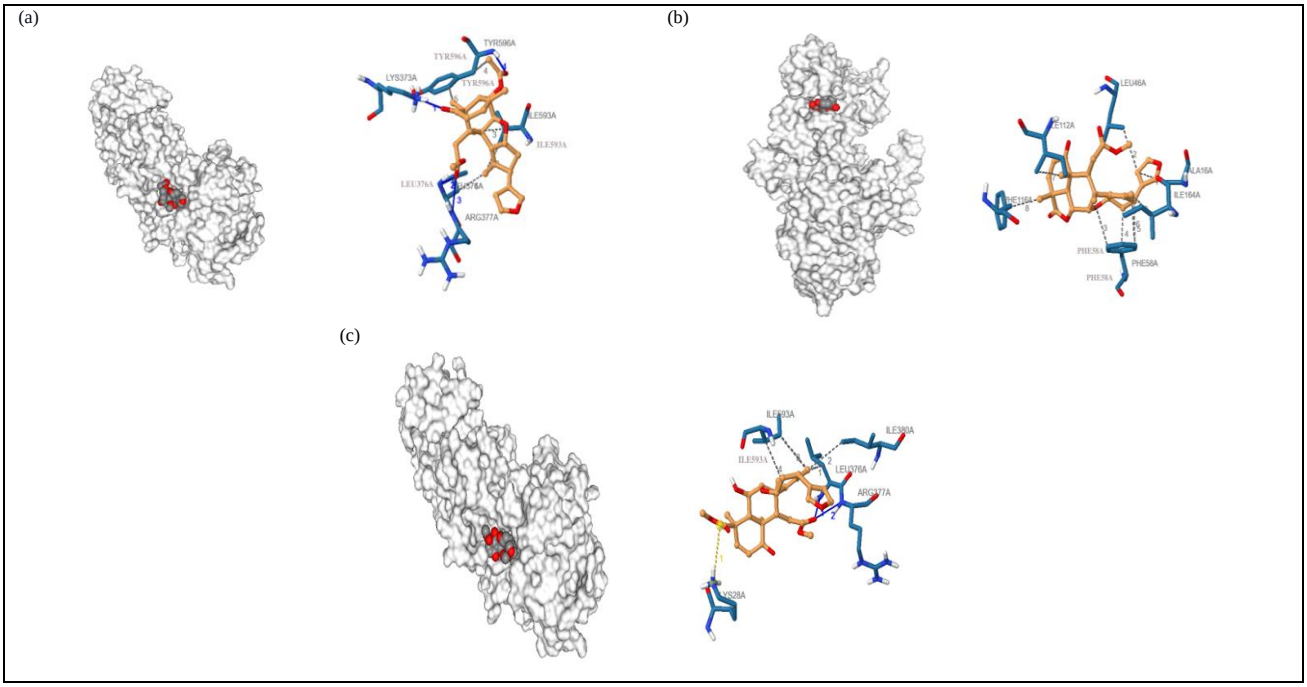

Figure 3. The binding configuration of Nimbinene 3(a), Nimbolide 3(b), and Desacetylnimbin 3(c) in the *pf*DHFR-TS active site as obtained from molecular docking using AutoDock Vina. Binding interactions were analyzed using a protein-ligand interaction profiler. Blue dashed line - Hydrogen bond; Green dotted line – Pi stacking; Grey dotted line – Hydrophobic interaction.

All the compounds with the exemption of Emetine have an Enzyme inhibitor greater than 0.0, which indicates that they are highly active, while Emetine shows moderate activity.

Pharmacokinetics properties prediction

During drug discovery and development, it is crucial to determine bioactive compounds' absorption, distribution, metabolism, excretion, and toxicity (ADMET) properties. Umar *et al*.[48] reported that a potent small ligand should reach its target in the body in great concentration to be effective. To behave in its therapeutic influence, it must remain in its bioactive nature for an extended period. **Table 4** shows the *in silico* ADMET profiling of the bioactive compounds and the control drugs. **Figure 6** shows the **2D** structure of the bioactive compounds and the control drugs.

Table 4. Predicted ADMET properties of compounds and control drug

S/N. Class	Properties	Pyridoxine	Luteolin	Vernomygdin	Vernomenin	Nimbinene	Nimbolide	Desacetylnimbin	Emetine	R-prunasin	Artemether	Lumefantrine
1. Absorption	BBB	Yes	No	Yes	Yes	Yes	Yes	Yes	No	No	Yes	Yes
	Caco-2 permeability	No	Yes	No	No	No	No	No	Yes	No	Yes	No
	Pgp-inhibitor	No	No	No	No	Yes	Yes	Yes	No	Yes	Yes	Yes
	Pgp-Substrate	No	No	No	No	Yes	Yes	Yes	Yes	No	No	No
2. Distribution	PPB	7.9%	106.6%	65.3%	86.1%	90.1%	98.1%	102.4%	74%	41.3%	90.7%	110%
	Sub-cellular localization	Mitochondria	Mitochondria	Mitochondria	Mitochondria	Mitochondria	Mitochondria	Mitochondria	lysosomes	Mitochondria	Mitochondria	lysosomes
3. Metabolism	CYP450 1A2 inhibition	No	Yes	No	No	No	No	No	No	No	Yes	Yes
	CYP450 3A4 inhibition	No	Yes	No	No	Yes	Yes	Yes	No	No	No	No
	CYP450 3A4 substrate	No	No	Yes	Yes	Yes	Yes	Yes	Yes	No	Yes	Yes
	CYP450 2C9 inhibition	No	No	No	No	No	No	No	No	No	No	No
	CYP450 2C9 substrate	No	No	No	No	No	No	No	No	No	No	No
	CYP450 2C19 inhibition	No	No	No	No	No	No	No	No	No	No	No
	CYP450 2D6 inhibition	No	No	No	No	No	No	No	No	No	No	Yes
	CYP450 2D6 substrate	No	No	No	No	No	No	No	Yes	No	No	Yes
	UGT catalyzed	Yes	Yes	No	Yes	No	No	Yes	No	Yes	No	Yes
4. Toxicity	Acute oral toxicity	Class III	Class II	Class III	Class I	Class III	Class III	Class III	Class III	Class III	Class IV	Class III
	hERG inhibitor	No	No	No	No	Yes	Yes	Yes	Yes	No	Yes	Yes
	Human hepatotoxicity	No	Yes	Yes	No	Yes	Yes	Yes	No	No	No	Yes
	Ames mutagenicity	No	No	No	No	No	No	No	No	No	No	No
	Carcinogens	No	No	No	No	No	No	No	No	No	No	No

BBB - blood-brain barrier, PPB - plasma protein binding, hERG - human ether-a-go-go.

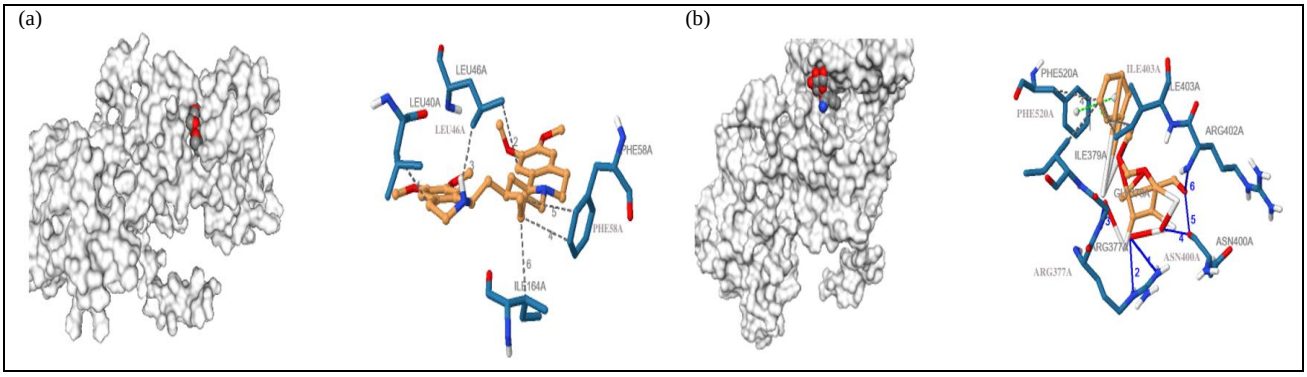

Figure 4. The binding configuration of Emetine 4(a), and (*R*)-prunasin 4(b), in the *pf*DHFR-TS active site as obtained from molecular docking using AutoDock Vina. Binding interactions were analyzed using a protein-ligand interaction profiler.

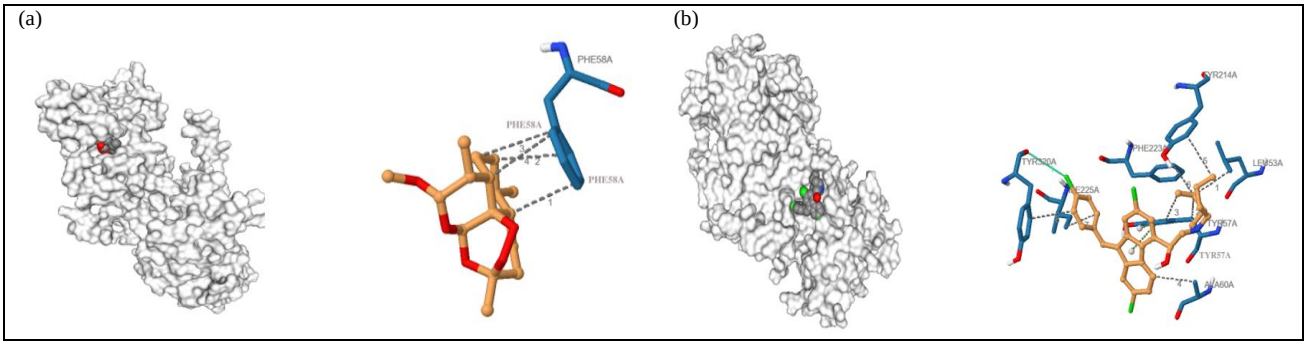

Figure 5. The binding configuration of Artemether 5(a), and Lumefantrine 5(b), in the *pf*DHFR-TS active site as obtained from molecular docking using AutoDock Vina. Binding interactions were analyzed using a protein-ligand interaction profiler.

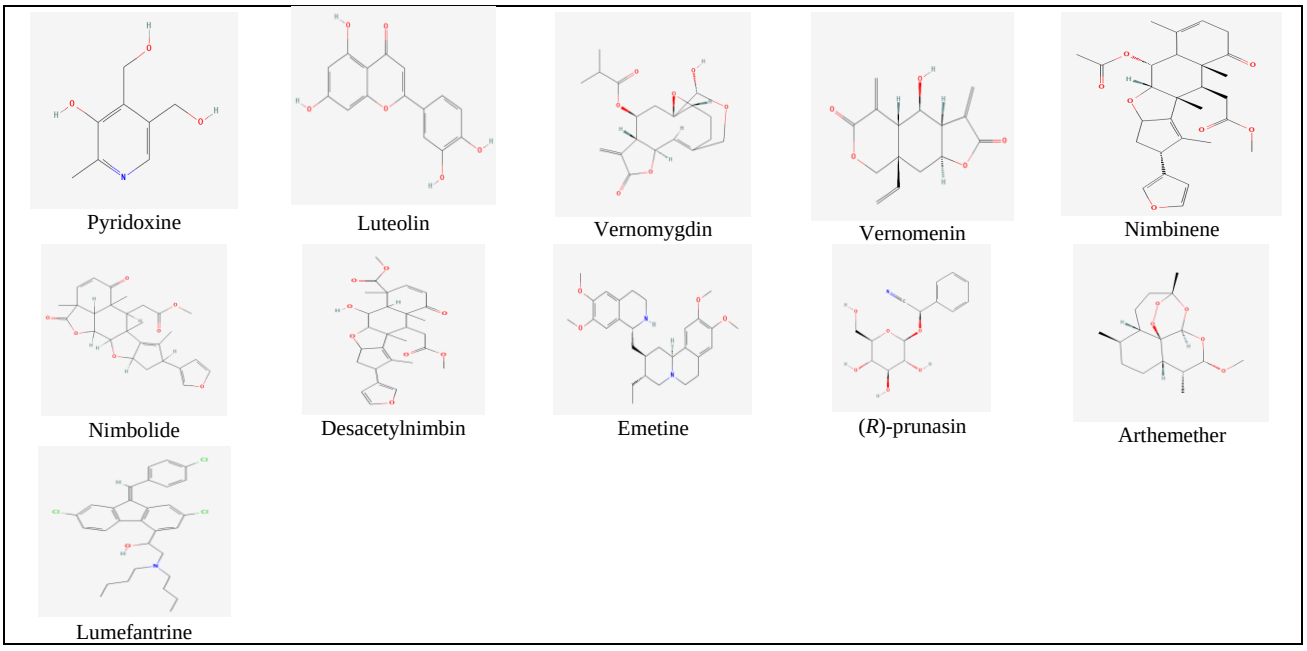

Figure 6. 2D structure of bioactive compounds and control drugs.

For drug absorption, all the top compounds except Luteolin, Emetine, and (*R*)-prunasin were predicted to penetrate the blood-brain barrier (BBB), and the control drugs also penetrate the blood-brain barrier (BBB). All the top compounds except Luteolin, Emetine, and Artemether have low absorption in the intestine through Caco-2 permeability. Most compounds were predicted to reside in mitochondria for drug distribution, while Emetine and Lumefantrine were localized in the lysosomes. For drug metabolism, all the compounds and the control drugs show no inhibition of some key enzymes (CYP2C9 and CYP450 2C19). Vernomygdin, Vernomenin, Nimbinene, Nimbolide, Desacetylnimbin, Emetine, Artemether, and Lumefantrine were substrates of CYP450 3A4, while Pyridoxine, Luteolin, and (*R*)-prunasin might likely inhibit CYP450 3A4 (as they were predicted as substrates). None of the compounds and the control drugs were found to be potential substrates of CYP450 2C9. For toxicity, Luteolin, Vernomygdin, Nimbinene, Nimbolide, Desacetylnimbin, and Lumefantrine were predicted to cause hepatotoxicity in humans. The compounds and the control drugs were predicted to show toxicity from the *Salmonella typhimurium* reverse mutation assay (AMES). None of the compounds and the control drugs were predicted to be carcinogenic.

DISCUSSION

Malaria is still a disease wreaking havoc on people's health, social lives, and economies in developing countries, including Nigeria. Despite developing various natural and synthetic antimalarial medications, it is still a leading cause of mortality as the parasites have evolved resistance against most currently used drugs. As a result, new medications are needed to overcome this resistance. Bioactive chemicals are employed directly as medications, or their bioactivity principles are utilized to produce novel pharmaceuticals. *In silico* methods predict bioactive compounds' efficacy and whether they can be used as drugs. Twenty (20) bioactive compounds from four African plants were subjected to *in silico* analysis in this study using *pf*DHFR-TS as the target protein to know their antimalarial properties. The bioactive compounds were compared with the control drugs, Artemether and Lumefantrine. The binding affinities of the bioactive compounds against the target protein *pf*DHFR-TS were calculated using PyRx software. The pharmacokinetic properties of the bioactive compounds and the biological activity were also predicted using online tools.

The bioactive compounds' and control drugs' drug-likeness properties in this study were evaluated using Lipinski's[32-34], Ghose's[35], Veber's[36], Egan's[37], and Muegge's[38] rules. Lipinski's rule of five considers the biological or pharmacological properties of a drug and determines its ability to make it an orally available drug[34]. Four out of the Lipinski's, Ghose's, Veber's, Egan's, and Muegge's rules were used in this present study to select the top hit from the bioactive compounds. In this study Pyridoxine, Luteolin, Vernomygdin, Vernomenin, Nimbinene, Nimbolide, Desacetylnimbin, Emetine, Carpaine, and (*R*)-prunasin passed four of the rules. The control drug Artemether didn't violate any rule, while Lumefantrine violated four out of the five rules. This study indicated that the bioactive compounds that passed the drug-likeness could be used as an oral drug. Using Lipinski's rule of five, all the nine (9) bioactive compounds and Artemether that passed this rule and had molecular weight within the Lipinski's range (≤500 Daltons), except Lumefantrine (528.94 daltons), as shown in **Table 1**. Lipinski's rule of five states that a drug compound with a molecular weight ≤500 Daltons has good druggability and can be used as a drug. This implies that all the bioactive compounds can be used as an oral drug[34] from the results presented in **Table 1**. The healing ability also depends on the drug's molecular weight. The surface area of the compound increases as the molecular weight increases beyond a specific limit, reducing the penetrability of the compound[33]. Other factors that determine the drug compounds' permeability and ultimately determine oral bioavailability are Molecular Lipophilicity Potential (XlogP value) and Topological Polar Surface Area (TPSA). XlogP is the logarithm of the n-octanol/water distribution coefficient. Molecular Lipophilicity Potential impacts membrane permeability and hydrophobic binding to macromolecules, including the target receptor and other proteins like plasma proteins, transporters, or metabolizing enzymes[49]. According to Lipinski's rule of five, if LogP< 5 indicates the drug compound prefers hydrophilic (polar) media, while the drug compound prefers hydrophobic (non-polar) media if LogP> 5[34]. In this current study, all the nine bioactive compounds (Luteolin, Vernomygdin, Vernomenin, Nimbinene, Nimbolide, Desacetylnimbin, Emetine, Carpaine, and (*R*)-prunasin) and Artemether have LogP value that is less than five. The compounds interacted well in hydrophilic (polar) media, while Lumefantrine has a value greater than 5 (8.72), which indicates that it interacts well in hydrophobic (non-polar) media.

The molecular docking analysis in this study revealed that Nimbolide derived from Neem leaf had the best binding affinity against all the targets compared to other ligands and the standard drug (**Table 2**). Nimbolide had binding energy of -10.1kcal/mol, followed by Vernomygdin derived from the bitter leaf, which had binding energy of -9.2kcal/mol, Luteolin derived from the bitter leaf, which had binding energy of -8.6kcal/mol, and Emetine derived from pawpaw leaf which had binding energy of -9.2kcal/mol. This binding interaction is better than that of the control drugs. Based on the shape and electrostatic interaction of the ligand and protein, the

molecular interaction predicts the binding conformation or pose of the ligand bound to the protein, which can be quantified[50]. The total number of interactions observed is estimated to be the ligand's docking score into the protein's binding pocket[50]. The docking score is expressed as a negative energy value in Kcal/mol, with the lower the negative total energy E indicating a stronger interaction between the ligands and the protein. The docking method predicts the best binding conformation of the compounds at the protein binding pocket and the interaction between the ligand and the residues at the enzyme's active site. The molecular docking in this study showed that Nimbolide, Vernomygdin, Luteolin, and Emetine have stronger interaction with the target protein, which can inhibit the effects caused by the *Plasmodium falciparum.*

Therefore, binding the bioactive compounds to the *Plasmodium falciparum* dihydrofolate reductase-thymidylate synthase (*pf*DHFR-TS) target may offer some anti-malarial benefits in treating malaria by inhibiting the target. It also shows the compounds' potential ability to bind to this target's catalytic sites. From this study, Nimbolide, Vernomygdin, Luteolin, and Emetine derived from Neem leaf, bitter leaf, and pawpaw, respectively, have a better binding to *pf*DHFR-TS than Artemether and Lumefantrine and could serve as potent inhibitors of this receptor which can serve as an anti-malarial drug. Thus, the ligand Nimbolide with the highest docking score shows the binding affinity with the amino acid residues at Ala16, Leu46, Phe58, Ile112, Phe116, and Ile164 using hydrophobic interaction (**Figure 3b**). Vernomygdin shows the binding affinity with the amino acid residues at Leu40, Leu46, Phe58, Ile112, and Tyr170 using hydrophobic interaction (**Figure 2c**). Luteolin shows the binding affinity with the amino acid residues at Gly44, Ile164, and Asp194, using hydrogen interaction, and shows the binding affinity with the amino acid residues at Leu40, Val195 using hydrophobic interaction (**Figure 2b**). Emetine shows the binding affinity with the amino acid residues at Leu40, Leu46, Phe58, and Ile164 using hydrophobic interaction (**Figure 4a**). The above residues act as a binding pocket for the ligand. Thus, Nimbolide, Vernomygdin, Luteolin, and Emetine derivatives will be more effective against *Plasmodium falciparum* dihydrofolate reductase-thymidylate synthase (*pf*DHFR-TS) than Artemether and Lumefantrine's control drugs. The binding of Nimbolide, Vernomygdin, Luteolin, and Emetine with *pf*DHFR-TS was observed to prevent the entry of any incoming substrate. The interaction of these compounds with this protein may limit cell proliferation, which is characteristic of malaria. It may reduce the adverse effects associated with this physiological process caused by *plasmodium*. Choowongkomon *et al.*[51], in their studies, show that Ala16, Leu40, Gly44, Leu46, Asp54, Phe58, Ser108, Ser111, Ile112, Ile164, Ser167, Tyr 170, Thr 185, and Val 195 are the interacting residues of DHFR with pyrimethamine. This current study also shows an analog interaction with residues such as Ala16, Leu40, Gly44, Leu46, Asp54, Phe58, Ile112, Ile164, and Tyr 170. The interaction of these residues may potentially minimize the resistance to malaria. The results from this study also show similar interaction of pyrimethamine with DHFR to inhibit the effects caused by malaria. Nimbolide, Vernomygdin, Luteolin, and Emetine Inhibition of *pf*DHFR-TS depends on their ability to form different bonds between the amino acid residue at the active site and the ligand. Also, the elimination of toxic effects that might result is due to the specificity of the compounds to interact with the amino acid residues at the active site of *pf*DHFR-TS. David *et al.* [50] reported that for an inhibition to occur in *pf*DHFR-TS, interaction is needed on some essential amino acid residue, including Asp54, Asn/Ser108, Ile /Leu164, and Ile14 at the active site of the protein. **Figure 2a** shows that Pyridoxine forms a hydrogen bond with Asp54. Luteolin also adopts hydrogen bond interaction with Ile164 at the binding pocket of the protein (**Figure 2b**). Nimbolide interacted with Ile164 using hydrophobic interaction (**Figure 3b**). Emetine interacted with Ile164 using hydrophobic interaction (**Figure 4a**). These interactions indicated the biological interaction of the compounds with *pf*DHFR-TS to show their potential inhibitor to *pf*DHFR-TS. Lipophilic, hydrogen bonding, and pi- stacking interactions are essential in protein-ligand interactions at the active site. Protein-ligand interactions highlighted the importance of lipophilic, electrostatic, and hydrogen bond interactions in protein-ligand interactions.

The pharmacological activity of drugs describes their beneficial effects on living beings and the availability of the drug to bind to a biological target. The most common biological targets are proteins such as enzymes, ion channels, and receptors. The biological target is also the drug target[46]. The bioactivity scores of the compounds were calculated for various parameters such as binding to GPCR and nuclear receptor ligands, ion channel modulation, kinase inhibition, protease inhibition, and enzyme activity inhibition. All parameters were calculated using the online software Molinspiration (www.molinspiration.com), which predicted that the synthesized complexes would have moderate biological activity[46]. The results obtained from this study indicated that Pyridoxine, Luteolin, Vernomygdin, Vernomenin, Nimbinene, Nimbolide, Desacetylnimbin, Emetine, (*R*)-prunasin, Artemether, and Lumefantrine do not have a bioactivity score less than -5.0 (< -5.0) which indicate they are all active to the binding to GPCR and nuclear receptor ligands, ion channel modulation, kinase inhibition, protease inhibition, and enzyme activity inhibition.

In the drug design and discovery process, it is essential to determine the target compounds' absorption, Distribution, Metabolism, Excretion, and Toxicity characteristics. These properties specify the pharmacological properties of the compounds and their ability to reach their target protein[52] and remain there for an extended period to exact its therapeutic influence. In our current study, the ADMET properties of the control drugs, the hit ligands, and the remaining ligands using the online server ADMETlab are the results in **Table 4**. The best four-hit, Nimbolide, Vernomygdin, Luteolin, and Emetine, showed excellent ADMET properties. The pharmacokinetic profile of the compounds shown in **Table 4** indicated that Nimbolide and Emetine are the only two hits that were P-glycoprotein substrates, and the two control drugs were not P-glycoprotein substrates. According to Lin *et al*.[53], P-glycoprotein is one of the ATP binding cassette (ABC) proteins involved in discharging molecules from the cell, preventing compounds from bioaccumulating, and eliciting their response; this implies the suitable drug property of Nimbolide and Emetine. Plasma protein binding is an essential mechanism of drug uptake and distribution (PPB). The pharmacodynamic behavior of drugs also depends on the binding of a drug to proteins in plasma. Drug oral bioavailability can be affected by PPB. When a drug binds to serum proteins in this process, the free concentration of the drug is at stake. A drug is considered to have a proper PPB if it has a predicted value of less than 90%, and medications with high protein bound may have a low therapeutic index. Vernomygdin and Emetine have *a* PPB value of less than 90%, which may indicate their high therapeutic index. Nimbolide, Vernomygdin, Luteolin, and Emetine do not inhibit some key liver enzymes CYP (**Table 4**). Cytochrome P450 (CYP) is an essential pharmacokinetic property (CYP), a family of enzymes that catalyze the phase 1 metabolism of xenobiotics at large. Esteves *et al*.[54] reported that any compound that inhibits selected isoforms would induce a drug-drug interaction. Nimbolide, Vernomygdin, Luteolin, and Emetine were predicted to non-inhibit the isoform CYP450 2C9, CYP450 2C19, and CYP450 2D6 and were expected to be non-inhibitors of these enzymes and cannot induce a drug-drug interaction, as loss of efficacy is the consequence of drug-drug interaction. Nimbolide, Vernomygdin, Luteolin, and Emetine were predicted to be non-carcinogenic and non-mutagenic and could be linked to the earlier outcome from the inflexible drug-likeness screening. The lead compounds were better than the control drugs, though there is a need for pharmacophoric modeling, which can improve some of the fundamental ADMET properties of the ligands. Carcinogenicity is of great concern among the toxicological endpoints of drugs. Any carcinogenic drugs may damage the genome or disrupt cellular metabolic processes in the human physiological system, affecting humans[49]. Non-carcinogenic properties of Nimbolide, Vernomygdin, Luteolin, and Emetine predicted their ability to be used as a drug. Thus, this current work indicates that the active compounds of these African plants, Nimbolide, Vernomygdin, Luteolin, and Emetine, may possess the most *in silico* inhibitory effect against *pf*DHFR-TS through a molecular docking technique. However, the outcomes of this study need to be validated using molecular dynamic simulation and other wet-lab studies.

CONCLUSION

The study revealed that nine (9) out of the bioactive compounds from four African plants, *Vernonia amygdalina* (Bitter leaf), *Cymbopogon citratus* (Lemongrass), *Azadirachta indica* (Neem leaf), and *Carica papaya* (Pawpaw leaf) passed the drug-likeness screening (Pyridoxine, Luteolin, Vernomygdin, Vernomenin, Nimbinene, Nimbolide, Desacetylnimbin, Emetine, (*R*)-prunasin), which shows their ability to serve as a drug. The study indicated that eleven (11) out of the twenty bioactive compounds violated two or more of the five rules Lipinski's, Ghose's, Veber's, Egan's, and Muegge's. Lumefantrine violated four of the five rules compared to the other bioactive compounds. Furthermore, the molecular docking of the ligands with the *pf*DHFR-TS protein shows that Nimbolide, Vernomygdin, Luteolin, and Emetine from *Azadirachta indica* (Neem leaves), *Vernonia amygdalina* (Bitter leaf), and *Carica papaya* (Pawpaw leaf) have lower binding energy than Artemether and Lumefantrine. This predicts their binding affinity to *pf*DHFR-TS and suggests they may possess antimalarial activity. From the present study, it is concluded that compounds from *Azadirachta indica* (Neem leaves), *Vernonia amygdalina* (Bitter leaf), and *Carica papaya* (Pawpaw leaf) show better docking with the target protein compared to Artemether and Lumefantrine, these bioactive compounds may inhibit the target protein *pf*DHFR-TS which is essential for malaria treatment. Further experimental assessment of biological activity is recommended for the validation of the computational results of the hit compounds

Funding Acknowledgment

No external funding was received.

Conflict of interest

The authors declare that there is no conflict of interest regarding the publication of this paper.

REFERENCES

1. Vogel, G. Infectious disease - new map illustrates risk from the 'other'malaria. *Science*. **2010**, *329*, 618–618.

2. Hoffman, S.L.; Subramanian, G.M.; Collins, F.H.; Venter, J.C. *Plasmodium*, human and Anopheles genomics and malaria. *Nature* **2002**, 415, 702–709.
3. White, N.J. Antimalarial drug resistance. *J. Clin. Invest*. **2004**, *113*, 1084–1092.
4. Anthony, M.P.; Burrows, J.N.; Duparc, S.; Moehrle, J.; Wells, T.N.C. The global pipeline of new medicines for the control and elimination of malaria. *Malaria J*. **2012**, *11*, 316.
5. World Health Organization (WHO). *Artemisinin Resistance and Artemisinin-Based Combination therapy Efficacy*, WHO, Geneva, Switzerland, http://apps.who.int/iris/bitstream/handle/10665/274362/WHO-CDS-GMP 2018.18-eng.pdf.
6. Anderson, A. Targeting DHFR in parasitic protozoa. *Drug Discovery Today*. **2005**, *10* (2):121–128.
7. Tse, E. G.; Korsik, M.; Todd, M. H. The past, present and future of anti-malarial medicines. *Malaria J*. **2019**, *18* (1), 93.
8. Zhang, K.; Rathod, P. K.; Divergent Regulation of Dihydrofolate Reductase between Malaria Parasite and Human Host. *Science*. **2013**, *296* (5567), 545– 547.
9. Oladele, T.O.; Bewaji, C.O.; and Sadiku, J. S. Drug target selection for malaria: molecular basis for the drug discovery process. *Centrepoint Journal (Science Edition)*. **2012**, *18* (2) 111–124.
10. Sullivan, D.J.; Kaludov, N.; Martinov, M.N. Discovery of potent, novel, non-toxic anti-malarial compounds via quantum modelling, virtual screening and in vitro experimental validation. *Malar J*. **2011**, *10*, 274.
11. Cronin, M.T.D. Computer-assisted prediction of drug toxicity and metabolism in modern methods of drug discovery. In: Hilgenfeld R, Hillisch A (eds) Modern methods of drug discovery. Birkhäuser, Basel, **2003**.
12. Yuan, H.; Ma, Q.; Ye, L.; and Piao, G. The traditional medicine and modern medicine from natural products. *Molecules* **2016**, *21* (5), 559.
13. Muschietti, L.; Vila, R.; Filho, V.C.; and Setzer, W. Tropical protozoan diseases: natural product drug discovery and development. *Evidence-Based Complementary and Alternative Medicine*. **2013**, *Article* ID 404250, 2 pages.
14. Ijeh, I.I.; Ejike, C.E.; C.C. Current perspectives on the medicinal potentials of *Vernonia amygdalina Del*. *J. Med Plants Res*. **2011**, *5*(7), 1051-1061.
15. Odeh, A.P.; Usman, A.A. Antimalarial activity and phytochemical analysis of aqueous leaf extract of *Vernonia amygdalina*. *J. Zool. Biosci. Res*. **2014**, 3, 28-31.
16. Olorunnisola, S. K.; Asiyanbi, H. T.; Hammed, A. M.; Simsek S. Biological properties of lemongrass: An overview. *Int. Food Res. J.* **2014**, *21* (2), 455-462.
17. Promila and Madan V. K. A Review on the Phytochemistry and Pharmacology of *Cymbopogon citratus Stapf*. (Lemongrass). *Pharm. Innovation J*. **2018**, *7* (3), 300-304.
18. Shakib, U. Pharmacological activities of neem (*Azadirachta indica*): A review. *Int. J. Pharmacognosy Life Sci*. **2020**, *1* (1). 38-41. https://doi.org/10.33545/27072827.2020.v1.i1a.8.
19. Budiarti, M.; Maruzy, A.; Mujahid, R.; Sari, A. N.; Jokopriyambodo, W.; Widayat, T.; Wahyono, S. The use of antimalarial plants as traditional treatment in Papua Island, Indonesia. *Heliyon*. **2020**, *6* (12), e05562. https://doi.org/10.1016/j.heliyon.2020.e05562.
20. Yogiraj, V.; Goyal, P.K.; Chauhan, C.S. *Carica papaya* linn: an overview. *Int. J. Herb. Med.* **2015**, *2* (5), 18.
21. Teng, W.C.; Chan, W.; Suwanarusk, R.; Ong, A.; Ho, H.K.; and Russell, B. In Vitro antimalarial evaluation and cytotoxicity investigations of *Carica papaya* leaves and carpaine. *Nat. Prod. Commun*. **2019**, *14* (1), 33–36.
22. Meng, X.Y.; Zhang, H.X.; Mezei, M.; and Cui, M. Molecular docking: a powerful approach for structure-based drug discovery. *Current Computer Aided-Drug Design*. **2011**, *7* (2). 146–157.
23. Alara, O.R.; Abdurahman, N.H.; Abdul Mudalip, S.K.; Olalere, O.A. Phytochemical and Pharmacological Properties of *Vernonia amygdalina*: a review. *J. Chem. Engin. Indust. Biotechnol*. **2017**, V2. 80-96. DOI: https://doi.org/10.15282/JCEIB-V2-07.29/9/2017/2.2.
24. Majewska, E.; Koz owska, M.; Gruczy ska-S kowska, E.; Kowalska, D.; Tarnowska, K. Lemongrass (*Cymbopogon citratus*) Essential Oil: Extraction, Composition, Bioactivity and Uses for Food Preservation - a Review. *Pol. J. Food Nutr. Sci*. **2019**, *69* (4). 327-341. DOI: 10.31883/pjfns/113152 http://journal.pan.olsztyn.pl.
25. Mohammad, MS.; Forough, M. Investigation of Compounds from *Azadirachta indica* (Neem). *Asian J. Plant Sci*. **2007**, *6* (2), 444 - 445.
26. Sofia, E.R.; Sulisetijono, and Umie, L. Phytochemical Screening, Antioxidant Activity, and Total Phenol Profile of *Carica pubescens* Leaves from Cangar, Batu- East Java, Indonesia. *International Conference on Life Sciences and Technology*. **2019**, 276, 1 -7. doi:10.1088/1755-1315/276/1/012022.
27. Kim, S.; Chen, J.; Cheng, T.; Gindulyte, A.; He, J.; He, S.; Li, Q.; Shoemaker, B. A.; Thiessen, P. A.; Yu, B.; Zaslavsky, L.; Zhang, J.; & Bolton, E. E; . PubChem in 2021: new data content and improved web interfaces. *Nucleic Acids Res.* **2019**, *49*(D1),

D1388–D1395. https://doi.org/10.1093/nar/gkaa971.
28. Yuthavong, Y.; Yuvaniyama, J.; Chitnumsub, P.; Xvanichtananku, P.; Chusacultanachai, S.; Tarnchompoo, B.; Vilaivan, T.; and Kamchonwongpaisan, S. Malarial (*Plasmodium falciparum*) dihydrofolate reductase-thymidylate synthase: structural basis for antifolate resistance and development of effective inhibitors. *Parasitology*. **2005**, 130, 249–259. DOI: 10.1017/S003118200400664X.
29. Berman, H.M.; Westbrook,J.; Feng,Z.; Gilliland,G.; Bhat, T.N.; Weissig,H., Shindyalov, I.N.; Bourne,P.E. The Protein Data Bank *Nucleic Acids Research*. **2000**, 28: 235-242.
30. Pettersen, E.F.; Goddard, T.D.; Huang, C.C.; Couch, G.S.; Greenblatt, D.M.; Meng, E.C.; and Ferrin, T.E. UCSF Chimera--a visualization system for exploratory research and analysis. . *J Comput Chem.* **2004**, 25(13):1605-12.
31. Daina, A.; Michielin, O.; & Zoete, V. SwissADME: a free web tool to evaluate pharmacokinetics, drug-likeness and medicinal chemistry friendliness of small molecules. *Sci Rep*. **2017**. 7, 42717. https://doi.org/10.1038/srep42717.
32. Lipinski, C. Rule of five in 2015 and beyond: Target and ligand structural limitations, ligand chemistry structure and drug discovery project decisions. *Adv. Drug Deliv. Rev*. **2016**, *101*, 34–41.
33. Lipinski, C.A. Drug-like properties and the causes of poor solubility and poor permeability. *J Pharmacol Toxicol Methods*. **2008**, 44:235–249
34. Lipinski, C.A.; Lombardo, F.; Dominy, B.W.; Feeney, P.J. Experimental and computational approaches to estimate solubility and permeability in drug discovery and development settings. *Adv. Drug Delivery Rev*. **2001**, 46(1-3):3–26. https://doi.org/10.1016/S0169-409X(00)00129-0.
35. Bickerton, G.R.; Paolini, G.V.; Besnard, J.; Muresan, S.; & Hopkins, A. L.;. Quantifying the chemical beauty of drugs. *Nature chemistry*. **2012**, *4*(2), 90–98.https://doi.org/10.1038/nchem.1243.
36. Veber, D.F.; Johnson, S.R.; Cheng, H.Y.; Smith, B.R.; Ward, K.W.; Kopple, K.D. Molecular Properties That Influence the Oral Bioavailability of Drug Candidates. *J. Med. Chem*. **2002**, 45, 2615–2623.
37. Egan, W. J.; Merz, K. M.; & Baldwin, J. J.; Prediction of Drug Absorption Using Multivariate Statistics. *J. Med. Chem.* 2000, **43**, 3867–3877.
on a comprehensively collected ADMET database. *J. Cheminform* **2018**, *10* (1), 29. https://doi.org/10.1186/s13321-018-0283-x.
48. Umar, H.I; Josiah, S.S.; Saliu, T.P.; Jimoh, T.O.; Ajayi, A.; and Danjuma, J.B. In-silico analysis of the inhibition of the SARS-CoV-2 main protease by
38. Muegge, I.; Heald, S.L.; Brittelli, D. Simple Selection Criteria for Drug-like Chemical Matter. *J. Med. Chem.* **2001**, *44*, 1841–1846.
39. Trott, O.; Olson, A.J. AutoDock Vina: improving the speed and accuracy of docking with a new scoring function, efficient optimization and multithreading. *J Comput Chem*. **2010**, 31(2):455–461.
40. Jarunee, V.; Supannee, T.; Chayasith, U.; Penchit, C.; Tirayut, V.; Yongyuth, Y.; and Sumalee, K. Combined Spatial Limitation around Residues 16 and 108 of *Plasmodium falciparum* Dihydrofolate Reductase Explains Resistance to Cycloguanil. *Antimicrobial Agents and Chemotherapy*. **2012**, 56(7). 3928–3935. DOI:10.1128/AAC.00301-12.
41. Zeeshan, I.; Mubashir, H.; Jawaria, M.; Irfana, M.; Farah, R.S.; Abdul Rauf, S.; and Nasir-ud-Din. Identification of Novel Dihydrofolate Reductase Inhibitor as Potential Antimalarial Drug: *In silico* Studies. *Pakistan J. Zool.* **2014**, *46* (5), 1263-1270.
42. Delano. The PyMOL molecular graphics system, DeLano Scientific LLC, 400 Oyster Point Blvd., Suite 213, South San Francisco, **2005**. CA 94080-1918, http://pymol.sourceforge.net.
43. Salentin, S.; Schreiber, S.; Haupt, V. J.; Adasme, M. F.; & Schroeder, M. PLIP: fully automated protein-ligand interaction profiler. *Nucleic acids research*. **2015**, *43*(W1), W443–W447. https://doi.org/10.1093/nar/gkv315.
44. Stierand, K.; Maass, P. C.; Rarey, M., Molecular complexes at a glance: automated generation of two-dimensional complex diagrams. *Bioinformatics*. **2006**, 22 (14), 1710-6. DOI: https://doi.org/10.1093/bioinformatics/btl150.
45. Fricker, P. C.; Gastreich, M.; Rarey, M., Automated drawing of structural molecular formulas under constraints. *J Chem Inf. Comput Sci*. **2004**, 44 (3), 1065-78. DOI: https://doi.org/10.1021/ci049958u.
46. Khan, T.; Dixit, S.; Ahmad, R.; Raza, S.; Azad, I.; Joshi, S.; & Khan, A. R. Molecular docking, PASS analysis, bioactivity score prediction, synthesis, characterization and biological activity evaluation of a functionalized 2-butanone thiosemicarbazone ligand and its complexes. *J. Chem. Biol.* **2017**, *10* (3), 91–104. https://doi.org/10.1007/s12154-017-0167-y.
47. Dong, J.; Wang, N. N.; Yao, Z. J.; Zhang, L.; Cheng, Y.; Ouyang, D.; Lu, A. P.; & Cao, D. S. ADMETlab: a platform for systematic ADMET evaluation based

some active compounds from selected African plants. *J Taibah Univ Med Sci*. **2021**, *16* (2), 162–76. https:// doi. org/ 10. 1016/j.jtumed. 2020. 12. 005.
49. Guo-Li, X.; Zhen-Xing, W.; Jia-Cai, Y.; Li Fu, Zhi-Jiang, Y.; Chang-Yu, H.; Ming-Zhu, Y.; Xiang-

Xiang, Z.; Cheng-Kun, W.; Ai-Ping, L.; Xiang, C.; Ting-Jun, H.; Dong-Sheng, C.; ADMETlab 2.0: an integrated online platform for accurate and comprehensive predictions of ADMET properties. *Nucleic Acids Res.*. **2021**, 49, 5 -14.

50. David, T.1.; Adelakun, N.S.; Omotuyi, O.I.; Metibemu, D.S.; Ekun, O.E.; Eniafe, G.O.; Inyang, O.K.; Adewumi, B.; Enejoh, O.A.; Owolabi, R.T.; Oribamis, E.I. Molecular docking analysis of phyto-constituents from *Cannabis sativa* with *pfDHFR*. *Bioinformation*. **2018**, *14* (9), 574-579.
51. Choowongkomon, K.; Theppabutr, S.; Songtawee, N.; Day, N.P.; White, N.J.; Woodrow, C.J.; and Imwong, M. Computational analysis of binding between malarial dihydrofolate reductases and anti-folates. *Malar. J*. **2010**, 9, 65.
52. Balogun, T.A.; Omoboyowa, D.A.; and Saibu, O.A. In silico Anti-malaria Activity of Quinolone Compounds against *Plasmodium falciparum* Dihydrofolate Reductase (*pf*DHFR), *International J. Biochem. Res. Rev*. **2020**, *29* (8), 10-17.
53. Lin, J; Yamazaki, M. Role of P-glycoprotein in pharmacokinetics. *Clin Pharmacokinet*. **2003**, *42* (1), 59–98.
54. Esteves, F.; Rueff, J.; Kranendonk, M. The central role of cytochrome P450 in xenobiotic metabolism—a brief review on a fascinating enzyme family. *J Xenobiot*. **2021**, *11* (3), 94–114.